

First Observation of the Decay $B \rightarrow J/\psi \phi K$

A. Anastassov,¹ J. E. Dubocq,¹ K. K. Gan,¹ C. Gwon,¹ T. Hart,¹ K. Honscheid,¹ D. Hufnagel,¹ H. Kagan,¹ R. Kass,¹ J. Lorenc,¹ T. K. Pedlar,¹ H. Schwarthoff,¹ E. von Toerne,¹ M. M. Zoeller,¹ S. J. Richichi,² H. Severini,² P. Skubic,² A. Undrus,² S. Chen,³ J. Fast,³ J. W. Hinson,³ J. Lee,³ N. Menon,³ D. H. Miller,³ E. I. Shibata,³ I. P. J. Shipsey,³ V. Pavlunin,³ D. Cronin-Hennessy,⁴ Y. Kwon,^{4,*} A.L. Lyon,⁴ E. H. Thorndike,⁴ C. P. Jessop,⁵ H. Marsiske,⁵ M. L. Perl,⁵ V. Savinov,⁵ D. Ugolini,⁵ X. Zhou,⁵ T. E. Coan,⁶ V. Fadeyev,⁶ I. Korolkov,⁶ Y. Maravin,⁶ I. Narsky,⁶ R. Stroynowski,⁶ J. Ye,⁶ T. Wlodek,⁶ M. Artuso,⁷ R. Ayad,⁷ C. Boulahouache,⁷ K. Bukin,⁷ E. Dambasuren,⁷ S. Karamov,⁷ S. Kopp,⁷ G. Majumder,⁷ G. C. Moneti,⁷ R. Mountain,⁷ S. Schuh,⁷ T. Skwarnicki,⁷ S. Stone,⁷ G. Viehhauser,⁷ J.C. Wang,⁷ A. Wolf,⁷ J. Wu,⁷ S. E. Csorna,⁸ I. Danko,⁸ K. W. McLean,⁸ Sz. Márka,⁸ Z. Xu,⁸ R. Godang,⁹ K. Kinoshita,^{9,†} I. C. Lai,⁹ S. Schrenk,⁹ G. Bonvicini,¹⁰ D. Cinabro,¹⁰ L. P. Perera,¹⁰ G. J. Zhou,¹⁰ G. Eigen,¹¹ E. Lipeles,¹¹ M. Schmittler,¹¹ A. Shapiro,¹¹ W. M. Sun,¹¹ A. J. Weinstein,¹¹ F. Würthwein,^{11,‡} D. E. Jaffe,¹² G. Masek,¹² H. P. Paar,¹² E. M. Potter,¹² S. Prell,¹² V. Sharma,¹² D. M. Asner,¹³ A. Eppich,¹³ J. Gronberg,¹³ T. S. Hill,¹³ D. J. Lange,¹³ R. J. Morrison,¹³ H. N. Nelson,¹³ R. A. Briere,¹⁴ B. H. Behrens,¹⁵ W. T. Ford,¹⁵ A. Gritsan,¹⁵ J. Roy,¹⁵ J. G. Smith,¹⁵ J. P. Alexander,¹⁶ R. Baker,¹⁶ C. Bebek,¹⁶ B. E. Berger,¹⁶ K. Berkelman,¹⁶ F. Blanc,¹⁶ V. Boisvert,¹⁶ D. G. Cassel,¹⁶ M. Dickson,¹⁶ P. S. Drell,¹⁶ K. M. Ecklund,¹⁶ R. Ehrlich,¹⁶ A. D. Foland,¹⁶ P. Gaidarev,¹⁶ L. Gibbons,¹⁶ B. Gittelman,¹⁶ S. W. Gray,¹⁶ D. L. Hartill,¹⁶ B. K. Heltsley,¹⁶ P. I. Hopman,¹⁶ C. D. Jones,¹⁶ D. L. Kreinick,¹⁶ M. Lohner,¹⁶ A. Magerkurth,¹⁶ T. O. Meyer,¹⁶ N. B. Mistry,¹⁶ C. R. Ng,¹⁶ E. Nordberg,¹⁶ J. R. Patterson,¹⁶ D. Peterson,¹⁶ D. Riley,¹⁶ J. G. Thayer,¹⁶ P. G. Thies,¹⁶ B. Valant-Spaight,¹⁶ A. Warburton,¹⁶ P. Avery,¹⁷ C. Prescott,¹⁷ A. I. Rubiera,¹⁷ J. Yelton,¹⁷ J. Zheng,¹⁷ G. Brandenburg,¹⁸ A. Ershov,¹⁸ Y. S. Gao,¹⁸ D. Y.-J. Kim,¹⁸ R. Wilson,¹⁸ T. E. Browder,¹⁹ Y. Li,¹⁹ J. L. Rodriguez,¹⁹ H. Yamamoto,¹⁹ T. Bergfeld,²⁰ B. I. Eisenstein,²⁰ J. Ernst,²⁰ G. E. Gladding,²⁰ G. D. Gollin,²⁰ R. M. Hans,²⁰ E. Johnson,²⁰ I. Karliner,²⁰ M. A. Marsh,²⁰ M. Palmer,²⁰ C. Plager,²⁰ C. Sedlack,²⁰ M. Selen,²⁰ J. J. Thaler,²⁰ J. Williams,²⁰ K. W. Edwards,²¹ R. Janicek,²² P. M. Patel,²² A. J. Sadoff,²³ R. Ammar,²⁴ P. Baringer,²⁴ A. Bean,²⁴ D. Besson,²⁴ R. Davis,²⁴ I. Kravchenko,²⁴ N. Kwak,²⁴ X. Zhao,²⁴ S. Anderson,²⁵ V. V. Frolov,²⁵ Y. Kubota,²⁵ S. J. Lee,²⁵ R. Mahapatra,²⁵ J. J. O'Neill,²⁵ R. Poling,²⁵ T. Riehle,²⁵ A. Smith,²⁵ J. Urheim,²⁵ S. Ahmed,²⁶ M. S. Alam,²⁶ S. B. Athar,²⁶ L. Jian,²⁶ L. Ling,²⁶ A. H. Mahmood,^{26,§} M. Saleem,²⁶ S. Timm,²⁶ and F. Wappler²⁶

(CLEO Collaboration)

¹Ohio State University, Columbus, Ohio 43210

²University of Oklahoma, Norman, Oklahoma 73019

³Purdue University, West Lafayette, Indiana 47907

⁴University of Rochester, Rochester, New York 14627

⁵Stanford Linear Accelerator Center, Stanford University, Stanford, California 94309

⁶Southern Methodist University, Dallas, Texas 75275

⁷Syracuse University, Syracuse, New York 13244

⁸Vanderbilt University, Nashville, Tennessee 37235

⁹Virginia Polytechnic Institute and State University, Blacksburg, Virginia 24061

¹⁰Wayne State University, Detroit, Michigan 48202

¹¹California Institute of Technology, Pasadena, California 91125

¹²University of California, San Diego, La Jolla, California 92093

¹³University of California, Santa Barbara, California 93106

¹⁴Carnegie Mellon University, Pittsburgh, Pennsylvania 15213

¹⁵University of Colorado, Boulder, Colorado 80309-0390

¹⁶Cornell University, Ithaca, New York 14853

¹⁷University of Florida, Gainesville, Florida 32611

¹⁸Harvard University, Cambridge, Massachusetts 02138

¹⁹University of Hawaii at Manoa, Honolulu, Hawaii 96822

²⁰University of Illinois, Urbana-Champaign, Illinois 61801

²¹Carleton University, Ottawa, Ontario, Canada K1S 5B6

and the Institute of Particle Physics, Canada

²²McGill University, Montréal, Québec, Canada H3A 2T8

and the Institute of Particle Physics, Canada

²³Ithaca College, Ithaca, New York 14850

²⁴University of Kansas, Lawrence, Kansas 66045

²⁵University of Minnesota, Minneapolis, Minnesota 55455

²⁶State University of New York at Albany, Albany, New York 12222

(January 8, 2022)

We present the first observation of the decay $B \rightarrow J/\psi \phi K$. Using 9.6×10^6 $B\bar{B}$ meson pairs collected with the CLEO detector, we have observed 10 fully reconstructed $B \rightarrow J/\psi \phi K$ candidates, whereas the estimated background is 0.5 ± 0.2 events. We obtain a branching fraction of $\mathcal{B}(B \rightarrow J/\psi \phi K) = (8.8_{-3.0}^{+3.5}[\text{stat}] \pm 1.3[\text{syst}]) \times 10^{-5}$. This is the first observed B meson decay requiring the creation of an additional $s\bar{s}$ quark pair.

An observation of a B meson decay requiring the creation of an additional $s\bar{s}$ quark pair in the final state would enhance our understanding of strong interactions in the final states of B decays. Previous studies of such processes involved searches for the “lower vertex” $\bar{B} \rightarrow D_s^+ X$ transitions [1], however no signal was observed. The decay $B \rightarrow J/\psi \phi K$ [2] can occur only if an additional $s\bar{s}$ quark pair is created in the decay chain besides the quarks produced in the weak $b \rightarrow c\bar{c}s$ transition. The $B \rightarrow J/\psi \phi K$ transition most likely proceeds as a three-body decay (Fig. 1). Another possibility is that the $B \rightarrow J/\psi \phi K$ decay proceeds as a quasi-two-body decay in which the J/ψ and ϕ mesons are daughters of a hybrid charmonium state [3].

We searched for $B^+ \rightarrow J/\psi \phi K^+$ and $B^0 \rightarrow J/\psi \phi K_S^0$ decays, reconstructing $J/\psi \rightarrow \ell^+ \ell^-$, $\phi \rightarrow K^+ K^-$, and $K_S^0 \rightarrow \pi^+ \pi^-$. Both $e^+ e^-$ and $\mu^+ \mu^-$ modes were used for the J/ψ reconstruction. The data were collected at the Cornell Electron Storage Ring (CESR) with two configurations of the CLEO detector, called CLEO II [4] and CLEO II.V. The components of the CLEO detector most relevant to this analysis are the charged particle tracking system, the CsI electromagnetic calorimeter, the time-of-flight system, and the muon chambers. In CLEO II, the momenta of charged particles are measured in a tracking system consisting of a 6-layer straw tube chamber, 10-layer precision drift chamber, and 51-layer main drift chamber, all operating inside a 1.5 T solenoidal magnet. The main drift chamber also provides a measurement of the specific ionization loss, dE/dx , used for particle identification. For CLEO II.V, the innermost wire chamber was replaced with a three-layer silicon vertex detector [5]. Muon identification system consists of proportional counters placed at various depths in the steel absorber.

*Permanent address: Yonsei University, Seoul 120-749, Korea.

†Permanent address: University of Cincinnati, Cincinnati OH 45221

‡Permanent address: Massachusetts Institute of Technology, Cambridge, MA 02139.

§Permanent address: University of Texas - Pan American, Edinburg TX 78539.

The results of this search are based upon an integrated luminosity of 9.1 fb^{-1} of $e^+ e^-$ data taken at the $\Upsilon(4S)$ energy and 4.4 fb^{-1} recorded 60 MeV below the $\Upsilon(4S)$ energy. The simulated event samples used in this analysis were generated using GEANT-based [6] simulation of the CLEO detector response. Simulated events were processed in a similar manner as the data.

When making requirements on such kinematic variables as invariant mass or energy, we took advantage of well-understood track and photon-shower covariance matrices to calculate the expected resolution for each combination. Therefore we extensively used normalized variables, which allowed uniform candidate selection criteria to be used for the data collected with the CLEO II and CLEO II.V detector configurations.

The normalized invariant mass distributions for the $J/\psi \rightarrow \ell^+ \ell^-$ signal in data are shown in Fig. 2. We required the normalized invariant mass to be from -10 to $+3$ (from -4 to $+3$) for the $J/\psi \rightarrow e^+ e^-$ ($J/\psi \rightarrow \mu^+ \mu^-$) candidates. The resolution in the $\ell^+ \ell^-$ invariant mass is about $10 \text{ MeV}/c^2$. To improve the energy and momentum resolution of a J/ψ candidate, we performed a fit constraining the mass of each J/ψ candidate to the world average value [7].

Electron candidates were identified based on the ratio of the track momentum to the associated shower energy in the CsI calorimeter and specific ionization loss in the drift chamber. The internal bremsstrahlung in the $J/\psi \rightarrow e^+ e^-$ decay as well as the bremsstrahlung in the detector material produce a long radiative tail in the $e^+ e^-$ invariant mass distribution and impede efficient $J/\psi \rightarrow e^+ e^-$ detection. We recovered some of the bremsstrahlung photons by selecting the photon shower with the smallest opening angle with respect to the direction of the e^\pm track evaluated at the interaction point, and then requiring this opening angle to be smaller than 5° . The addition of the bremsstrahlung photons resulted in a relative increase of approximately 25% in the $J/\psi \rightarrow e^+ e^-$ reconstruction efficiency without adding more background.

For the $J/\psi \rightarrow \mu^+ \mu^-$ reconstruction, one of the muon candidates was required to penetrate the steel absorber to a depth greater than 3 nuclear interaction lengths. We relaxed the absorber penetration requirement for the second muon candidate if it was not expected to reach a muon chamber either because its energy was too low or because it pointed to a region of the detector not covered by the muon chambers. For these muon candidates we required the ionization signature in the CsI calorimeter to be consistent with that of a muon. Muons typically leave a narrow trail of ionization and deposit approximately 200 MeV of energy in the crystal calorimeter. Hadrons, on the other hand, quite often undergo a nuclear interaction in the CsI crystals that have a depth of 80% of a nuclear interaction length. Compared to imposing the absorber penetration requirement on both muon

candidates, this procedure increased the $J/\psi \rightarrow \mu^+\mu^-$ reconstruction efficiency by 20% with 80% increase of background.

We required that the charged kaon candidates have dE/dx and, if available, time-of-flight measurements that lie within 3 standard deviations of the expected values.

If for the $B \rightarrow J/\psi \phi K$ decays we assume a uniform Dalitz distribution and isotropic decays of J/ψ and ϕ mesons, then the expected efficiency of the combined dE/dx and time-of-flight selection is approximately 90% per kaon candidate. The dE/dx measurements alone provide the K/π separation of more than 4 standard deviations for 92% of the ϕ daughter kaons and for 64% of the ‘‘bachelor’’ kaons from B decay. We selected $\phi \rightarrow K^+K^-$ candidates by requiring the K^+K^- invariant mass to be within 10 MeV/ c^2 of the ϕ mass [7]. We did not use the normalized K^+K^- invariant mass because the mass resolution (1.2 MeV/ c^2) is smaller than the ϕ width (4.4 MeV) [7].

The K_S^0 candidates were selected from pairs of tracks forming well-measured displaced vertices. The resolution in $\pi^+\pi^-$ invariant mass is about 4 MeV/ c^2 . We required the absolute value of the normalized $\pi^+\pi^-$ invariant mass to be less than 4, then we performed a fit constraining the mass of each K_S^0 candidate to the world average value [7].

The $B \rightarrow J/\psi \phi K$ candidates were selected by means of two observables. The first observable is the difference between the energy of the B candidate and the beam energy $\Delta E \equiv E(J/\psi) + E(\phi) + E(K) - E_{\text{beam}}$. The resolution in ΔE for the $B \rightarrow J/\psi \phi K$ candidates is approximately 6 MeV. The second observable is the beam-constrained B mass $M(B) \equiv \sqrt{E_{\text{beam}}^2 - p^2(B)}$, where $p(B)$ is the absolute value of the B candidate momentum. The resolution in $M(B)$ for the $B \rightarrow J/\psi \phi K$ candidates is about 2.7 MeV/ c^2 ; it is dominated by the beam energy spread. The distributions of the ΔE vs $M(B)$ for $B^+ \rightarrow J/\psi \phi K^+$ and $B^0 \rightarrow J/\psi \phi K_S^0$ are shown in Fig. 3. We used the normalized ΔE and $M(B)$ variables to select the $B \rightarrow J/\psi \phi K$ candidates and defined the signal region as $|\Delta E/\sigma(\Delta E)| < 3$ and $|(M(B) - M_B)/\sigma(M(B))| < 3$. We observed 8(2) events in the signal region for the $B^+ \rightarrow J/\psi \phi K^+$ ($B^0 \rightarrow J/\psi \phi K_S^0$) mode. Considering that K^0 can decay as K_S^0 or as K_L^0 , and also taking into account $\mathcal{B}(K_S^0 \rightarrow \pi^+\pi^-)$ and the difference in reconstruction efficiencies, we expect to observe on average 4.3 $B^+ \rightarrow J/\psi \phi K^+$ candidates for every $B^0 \rightarrow J/\psi \phi K_S^0$ candidate.

The Dalitz plot and the cosine of helicity angle distributions for the 10 $B \rightarrow J/\psi \phi K$ signal candidates are shown in Figs. 4 and 5. The helicity angle for $J/\psi \rightarrow \ell^+\ell^-$ decay is defined as the angle between a lepton momentum in the J/ψ rest frame and the J/ψ momentum in the B rest frame. An analogous definition was used for the $\phi \rightarrow K^+K^-$ decay. No conclusion can be drawn yet either about the J/ψ and the ϕ polarizations or about the resonant substructure of the

$B \rightarrow J/\psi \phi K$ decay. If the J/ψ and ϕ mesons are the products of the hybrid charmonium ψ_g decay, then the $J/\psi \phi$ invariant mass is expected to be below the DD^{**} threshold (4.3 GeV/ c^2) because $\psi_g \rightarrow DD^{**}$ decay is likely to dominate above the threshold [3]. The $J/\psi \phi$ invariant mass is above 4.3 GeV/ c^2 for all 10 $B \rightarrow J/\psi \phi K$ candidates thus disfavors the hybrid charmonium dominance scenario.

The background can be divided into two categories. First category is the combinatorial background from $\Upsilon(4S) \rightarrow B\bar{B}$ and continuum non- $B\bar{B}$ events. Second category is the background from non-resonant $B \rightarrow J/\psi K^+ K^- K$ decays.

The combinatorial background from $\Upsilon(4S) \rightarrow B\bar{B}$ events was estimated using a sample of simulated events approximately 32 times the data sample; events containing a $B \rightarrow J/\psi K^+ K^- K$ decay were excluded. We estimated the background from $\Upsilon(4S) \rightarrow B\bar{B}$ decays to be $0.25_{-0.08}^{+0.10}$ events. In addition, we specifically considered $B \rightarrow J/\psi K^* \pi^+$ with $K^* \rightarrow K\pi^-$ and $B \rightarrow J/\psi \rho^0 K$ decays because the beam-constrained B mass distribution for these modes is the same as for the $B \rightarrow J/\psi \phi K$ decays. Using data and simulated events, we verified that those backgrounds are rendered negligible by the kaon identification, ϕ mass, and ΔE requirements. The combinatorial background from the continuum non- $B\bar{B}$ events was estimated using simulated events and the data collected below $B\bar{B}$ threshold. We found the continuum background to be negligible.

To estimate the background contribution from the non-resonant $B \rightarrow J/\psi K^+ K^- K$ decays, we reconstructed $B^+ \rightarrow J/\psi K^+ K^- K^+$ and $B^0 \rightarrow J/\psi K^+ K^- K_S^0$ candidates in data requiring $|M(K^+K^-) - M_\phi| > 20$ MeV/ c^2 to exclude $B \rightarrow J/\psi \phi K$ events. We observed 7 $B \rightarrow J/\psi K^+ K^- K$ candidates with the estimated $B\bar{B}$ combinatorial background of 2.8 events. We estimated the mean background from $B \rightarrow J/\psi K^+ K^- K$ decays for the $B \rightarrow J/\psi \phi K$ signal to be $0.27_{-0.17}^{+0.21}$ events; we assumed that $B \rightarrow J/\psi K^+ K^- K$ decays according to phase space.

In summary, the estimated total background for the combined $B \rightarrow J/\psi \phi K$ signal is $0.52_{-0.19}^{+0.23}$ events.

We evaluated the reconstruction efficiency using a sample of simulated $B \rightarrow J/\psi \phi K$ decays. We assumed a uniform Dalitz distribution and isotropic decays of J/ψ and ϕ mesons; these assumptions are consistent with data (Figs. 4 and 5). The reconstruction efficiency, which does not include branching fractions of daughter particle decays, is $(15.5 \pm 0.2)\%$ for the $B^+ \rightarrow J/\psi \phi K^+$ mode and $(10.3 \pm 0.2)\%$ for the $B^0 \rightarrow J/\psi \phi K_S^0$ mode. The reconstruction efficiency is close to zero at the edges of phase space where either ϕ or K meson is produced nearly at rest in the laboratory frame. Thus, the overall detection efficiency would be much smaller than the above values if the $B \rightarrow J/\psi \phi K$ decay is dominated by either a $J/\psi K$ resonance with a mass around 4.3 GeV/ c^2

or a $J/\psi\phi$ resonance with a mass around $4.8 \text{ GeV}/c^2$. No such resonances are expected. To assign the systematic uncertainty due to the decay model dependence of the reconstruction efficiency, we generated two additional samples of simulated $B \rightarrow J/\psi\phi K$ events. One sample was generated with a uniform Dalitz distribution for $B \rightarrow J/\psi\phi K$ and 100% transverse polarization for J/ψ and ϕ . The other sample was generated assuming the ϕ and K mesons to be daughters of a hypothetical spin-0 resonance with mass $1.7 \text{ GeV}/c^2$ and width 100 MeV . We estimated the relative systematic uncertainty due to the decay model dependence of the reconstruction efficiency extraction to be 7%.

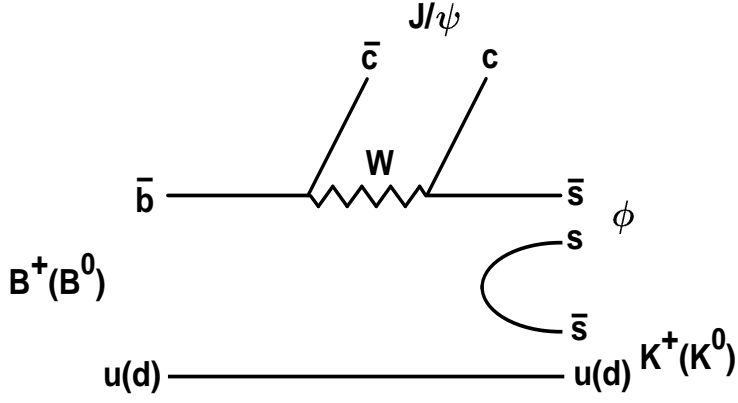
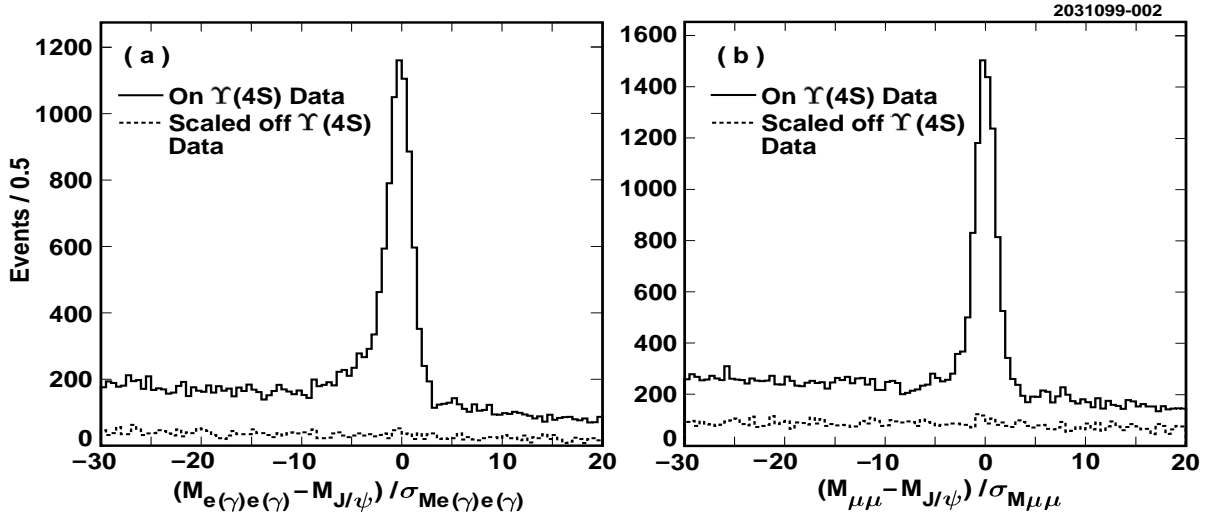
For the branching fraction calculation we assumed equal production of B^+B^- and $B^0\bar{B}^0$ pairs at the $\Upsilon(4S)$ resonance and $\mathcal{B}(B^+ \rightarrow J/\psi\phi K^+) = \mathcal{B}(B^0 \rightarrow J/\psi\phi K^0) = \mathcal{B}(B \rightarrow J/\psi\phi K)$. We did not assign any systematic uncertainty due to these two assumptions. We used the world average values of $\mathcal{B}(J/\psi \rightarrow \ell^+\ell^-)$, $\mathcal{B}(\phi \rightarrow K^+K^-)$, and $\mathcal{B}(K_S^0 \rightarrow \pi^+\pi^-)$ [7]. We used the tables in Ref. [8] to assign the 68.27% C.L. intervals for the Poisson signal mean given the total number of events observed and the known mean background. The resulting branching fraction is $\mathcal{B}(B \rightarrow J/\psi\phi K) = (8.8_{-3.0}^{+3.5}[\text{stat}] \pm 1.3[\text{syst}]) \times 10^{-5}$.

The systematic error includes the uncertainty in the reconstruction efficiency due to decay modeling plus the uncertainties in track finding, track fitting, lepton and charged-kaon identification, K_S^0 finding, background subtraction, uncertainty in the number of $B\bar{B}$ pairs used for this measurement, statistics of the simulated event samples, and the uncertainties on the daughter branching fractions $\mathcal{B}(J/\psi \rightarrow \ell^+\ell^-)$ and $\mathcal{B}(\phi \rightarrow K^+K^-)$ [7]. We estimated the total relative systematic uncertainty of the $\mathcal{B}(B \rightarrow J/\psi\phi K)$ measurement to be 15%.

In conclusion, we have fully reconstructed 10 $B \rightarrow J/\psi\phi K$ candidates with a total estimated background of 0.5 events. Assuming equal production of B^+B^- and $B^0\bar{B}^0$ pairs at the $\Upsilon(4S)$ resonance and $\mathcal{B}(B^+ \rightarrow J/\psi\phi K^+) = \mathcal{B}(B^0 \rightarrow J/\psi\phi K^0) = \mathcal{B}(B \rightarrow J/\psi\phi K)$, we have measured $\mathcal{B}(B \rightarrow J/\psi\phi K) = (8.8_{-3.0}^{+3.5}[\text{stat}] \pm 1.3[\text{syst}]) \times 10^{-5}$. This is the first observed B meson decay requiring the creation of an additional $s\bar{s}$ quark pair.

We gratefully acknowledge the effort of the CESR staff in providing us with excellent luminosity and running conditions. This work was supported by the National Science Foundation, the U.S. Department of Energy, the Research Corporation, the UTPA-Faculty Research Council Program, the Natural Sciences and Engineering Research Council of Canada, the A.P. Sloan Foundation, the Swiss National Science Foundation, and the Alexander von Humboldt Stiftung.

- [1] H. Albrecht *et al.* (ARGUS Collaboration), Z. Phys. **C60**, 11 (1993). X. Fu *et al.* (CLEO Collaboration), contribution to International Europhysics Conference on High Energy Physics (HEP 95) in Brussels, CLEO-CONF-95-11, EPS0169. A.F. Cho, Ph.D. dissertation, Cornell University, CLNS Thesis 97-1 (1997).
- [2] Charge conjugate modes are implied. $B \rightarrow J/\psi\phi K$ is either $B^+ \rightarrow J/\psi\phi K^+$ or $B^0 \rightarrow J/\psi\phi K^0$.
- [3] F.E. Close, I. Dunietz, P.R. Page, S. Veseli and H. Yamamoto, Phys. Rev. **D57**, 5653 (1998).
- [4] Y. Kubota *et al.* (CLEO Collaboration), Nucl. Instrum. Meth. **A320**, 66 (1992).
- [5] T.S. Hill, Nucl. Instrum. Meth. **A418**, 32 (1998).
- [6] R. Brun *et al.*, CERN Program Library Long Writeup W5013 (1993).
- [7] C. Caso *et al.*, Eur. Phys. J. **C3**, 1 (1998).
- [8] G.J. Feldman and R.D. Cousins, Phys. Rev. **D57**, 3873 (1998).

FIG. 1. Most likely $B \rightarrow J/\psi \phi K$ decay mechanism.FIG. 2. Normalized invariant mass of the (a) $J/\psi \rightarrow e^+e^-$ and (b) $J/\psi \rightarrow \mu^+\mu^-$ candidates in data. The solid line represents the data taken at the $\Upsilon(4S)$ energy; the dashed line represents the luminosity-scaled off resonance data showing the level of background from non- $B\bar{B}$ events.

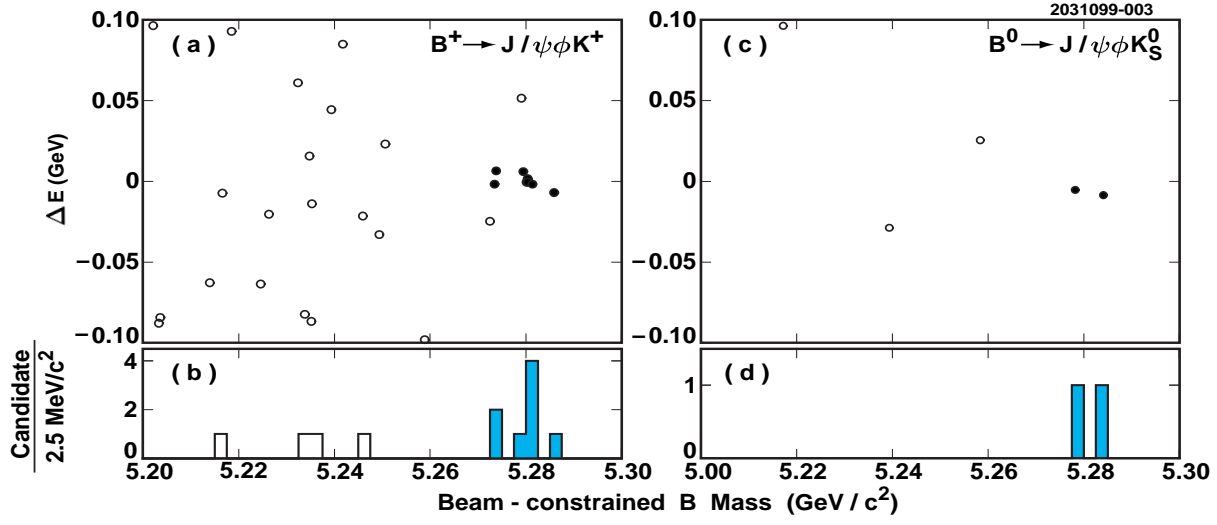


FIG. 3. The ΔE vs $M(B)$ distribution for (a) $B^+ \rightarrow J/\psi \phi K^+$ and (c) $B^0 \rightarrow J/\psi \phi K_S^0$ candidates in data. The signal candidates, selected using normalized ΔE and $M(B)$ variables, are shown by filled circles. The $M(B)$ distribution for (b) $B^+ \rightarrow J/\psi \phi K^+$ and (d) $B^0 \rightarrow J/\psi \phi K_S^0$ candidates satisfying $|\Delta E/\sigma(\Delta E)| < 3$; the shaded parts of the histograms represent signal candidates.

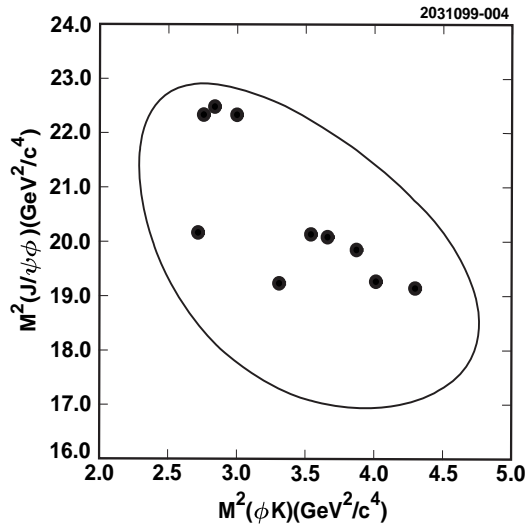


FIG. 4. Dalitz plot for the 10 $B \rightarrow J/\psi \phi K$ candidates in data. The kinematic boundary is represented by solid line.

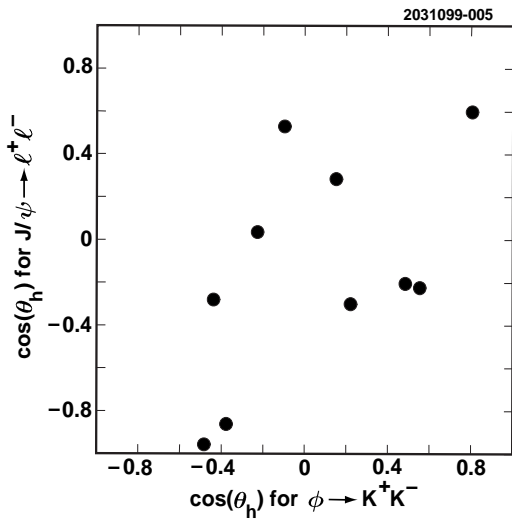


FIG. 5. The distribution of the cosine of helicity angle for $J/\psi \rightarrow \ell^+\ell^-$ vs the cosine of helicity angle for $\phi \rightarrow K^+K^-$ for the 10 $B \rightarrow J/\psi \phi K$ candidates in data.